Earth and Planetary Science Letters 620 (2023) 118317

Contents lists available at ScienceDirect

Earth and Planetary Science Letters

journal homepage: www.elsevier.com/locate/epsl

A Bayesian framework for subsidence modeling in sedimentary basins: A case study of the Tonian Akademikerbreen Group of Svalbard, Norway

Tianran Zhang [a,*], C. Brenhin Keller [a], Mark J. Hoggard [b], Alan D. Rooney [c], Galen P. Halverson [d], Kristin D. Bergmann [e], James L. Crowley [f], Justin V. Strauss [a]

[a] Department of Earth Sciences, Dartmouth College, Hanover, NH 03755, USA
[b] Research School of Earth Sciences, Australian National University, Canberra, Australia
[c] Department of Earth and Planetary Sciences, Yale University, New Haven, CT 06511, USA
[d] Department of Earth and Planetary Sciences, McGill University, Montréal, QC H3A 0E8, Canada
[e] Department of Earth, Atmospheric and Planetary Sciences, Massachusetts Institute of Technology, Cambridge, MA 02139, USA
[f] Department of Geosciences, Boise State University, Boise, ID 83725, USA

ARTICLE INFO

Article history:
Received 16 April 2023
Received in revised form 28 June 2023
Accepted 13 July 2023
Available online xxxx
Editor: A. Webb

Keywords:
age-depth modeling
Bayesian statistics
geochronology
Neoproterozoic

ABSTRACT

Quantitative subsidence analysis techniques have been widely utilized in ancient extensional basins to evaluate age relationships and unravel regional sedimentation patterns; however, uncertainties associated with various model inputs, such as lithological parameters, water depth, and relative or direct age uncertainties are often neglected. Here, we modify existing decompaction, backstripping and age-depth modeling procedures for post-rift thermally subsided basins through the introduction and propagation of uncertainties using both Monte Carlo and Markov chain Monte Carlo methods in a new program called SubsidenceChron.jl. As a case study for its potential utility in ancient extensional basins, we applied this technique to a globally relevant fossiliferous early Neoproterozoic (Tonian) sedimentary succession in northeastern Svalbard, Norway. Using two new geochronological constraints (Re-Os age from the Akademikerbreen Group and detrital zircon U-Pb maximum depositional age from the Veteranen Group) along with a published Re-Os age from the Polarisbreen Group and previously established age constraints for the onset of the Sturtian snowball Earth glaciation, our model generates a posterior stretching factor (β) of 1.29+0.08/−0.06 and a posterior thermal subsidence initiation time (t_0) of 840.40+18.64/−23.61 Ma. These results, along with the calculated age estimations for different stratigraphically important horizons throughout this succession, generally agree with those suggested by previous studies based on global chemostratigraphic correlations. The fewer assumptions made in our case study, as well as the incorporation and propagation of uncertainties on model inputs in SubsidenceChron.jl more broadly, contribute to important and quantifiable uncertainties in our age-depth model results. We suggest this approach will be relevant to future subsidence and age-depth models for Precambrian and Phanerozoic extensional sedimentary basins, in addition to providing a simple test of age models built solely on chemostratigraphic correlations.

1. Introduction

Sedimentary basins are areas on Earth's surface that produce accommodation space for sediment to accumulate and eventually transform into layered strata (Allen and Allen, 2013). Along with collisional and strike-slip basins, extensional basins (more commonly referred to as rift basins) are important sinks for sediment and commonly record tectonic events and paleoclimatic changes. To explain heat flow anomalies and stratigraphic patterns often observed in rift basins, McKenzie (1978) proposed a two-step, one-dimensional mathematical model for basins formed under stretching. The first step involved instantaneous and uniform rifting, resulting in subsidence caused by lithospheric thinning. The second part of the model predicted further subsidence driven by thermal relaxation of the mantle. Since McKenzie's (1978) initial rift model, numerous researchers have proposed variations upon this theme, capturing complex physical processes that occur in modern and ancient rift basins. For example, important modifications

* Corresponding author.
E-mail address: tianran.zhang.gr@dartmouth.edu (T. Zhang).

https://doi.org/10.1016/j.epsl.2023.118317
0012-821X/

include the evolution of extensional basins under finite (or protracted) stretching (e.g., Cochran, 1983; Jarvis and McKenzie, 1980; Pedersen and Ro, 1992), depth-dependent rifting (e.g., Beaumont et al., 1982; Davis and Kusznir, 2004; Huismans and Beaumont, 2014), or asymmetrical extension (e.g., Coward, 1986; Kusznir et al., 1991; Wernicke, 1981).

Building upon this theoretical framework for extensional basins, quantitative subsidence analysis techniques have been successfully utilized to explain the stratigraphic pattern and age-height/depth relationships in rifted basins. For example, the Mesozoic–Cenozoic subsidence history of the North Sea region has been analyzed in great detail with the aid of prolific geological and geophysical data (e.g., Japsen et al., 2007; Kooi et al., 1991; Sclater and Christie, 1980; Skogseid et al., 2000), and subsidence analyses on early Paleozoic rocks of the North American Cordillera have expanded these techniques to ancient rift basins (e.g., Bond et al., 1983; Bond and Kominz, 1984; Levy and Christie-Blick, 1991). Despite these foundational works, a critical aspect that has received relatively little attention in subsidence history reconstructions is the associated uncertainties. Specifically, the incorporation and propagation of uncertainties associated with various model inputs, such as age constraints and decompaction parameters, have commonly been absent. As a result, many subsidence models are unable to produce the entire range of possible outcomes. For Phanerozoic successions, this oversight may be less pronounced because of the effective use of biostratigraphy for providing age constraints. However, this approach becomes particularly problematic for Precambrian basins because they often do not host sufficient age information. Fortunately, recent advances in geochronological dating techniques, statistical modeling methods and computational performance provide a long-anticipated opportunity to develop a framework that treats uncertainties more robustly.

If uncertainties can be properly quantified, quantitative subsidence analysis techniques have great potential for establishing a more reliable Precambrian timescale (e.g., Shields et al., 2021). Halverson et al. (2018b, 2022) recently used a thermal-subsidence-derived age model for Tonian strata in northeastern Svalbard, Norway, to highlight the viability of previous global chemostratigraphic correlations for these strata. Despite suffering from a limited number of local radiometric ages, the composite Tonian sedimentary record from northeastern Svalbard published by Halverson et al. (2018a) is an ideal target to apply subsidence analysis age-depth modeling methods due to the relatively close spacing and small variability between individual measured sections that make up the composite stratigraphic section. Our research builds upon this work and aims to reexamine the age-depth relationship of the same succession with a modified approach. By using a recently published Re-Os age (Millikin et al., 2022) and new geochronologic data presented herein from the Svalbard Neoproterozoic succession, the age-depth relationship generated in this research is independent of chemostratigraphic age correlations. Moreover, our proposed age-depth modeling program can incorporate a suite of uncertainties by modeling the subsidence history using a Bayesian approach. Here we demonstrate the potential of this new approach as a useful tool for generating chronostratigraphic constraints in sedimentary basins, as well as its general utility in accurately incorporating uncertainties into standard basin analysis.

2. Methods

2.1. Subsidence modeling

We present a program named SubsidenceChron.jl (Zhang et al., 2023), available as a registered package written in the Julia programming language, to model subsidence and age-depth relationships within rift-related sedimentary basins. This program consists of two parts: 1) decompaction and backstripping, including the integration and propagation of uncertainties in compressibility and water depth; and 2) reconstructing the age-depth relationship during thermal subsidence using a Bayesian Markov chain Monte Carlo (MCMC) approach. The general workflow of this model is illustrated in Fig. 1, with more detailed explanations provided in the following subsections.

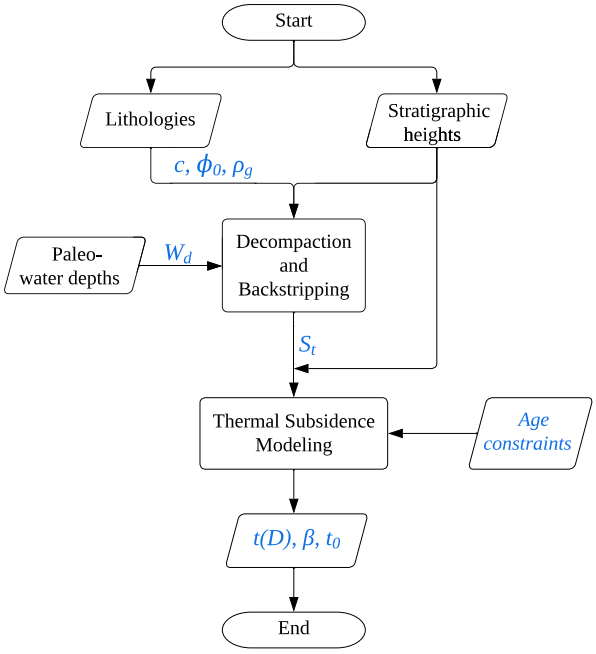

Fig. 1. Schematic workflow of SubsidenceChron.jl. Variables with uncertainties are italicized in blue. c = porosity-depth coefficient; ϕ_0 = surface porosity; ρ_g = grain density; W_d = paleo-water depth; S_t = tectonic subsidence; t(D) = age-depth relationship; β = stretching factor; t_0 = thermal subsidence initiation time.

2.1.1. Decompaction and backstripping

As the governing mathematical model behind SubsidenceChron.jl (Zhang et al., 2023), the McKenzie (1978) framework for post-rift thermal subsidence depicts the relationship between time and the amount of accommodation space created by tectonic forcings. Such accommodation space, also known as tectonic subsidence, can be derived from the thickness of the sediment column at the time of deposition through the removal of sediment and water loading. The stratigraphic thickness measured at present, however, is still an underestimation of the original thickness, mainly due to the process of mechanical compaction. To address this effect and tease out tectonic subsidence from the present-day stratigraphic thickness, decompaction and backstripping techniques are applied prior to modeling any age-depth relationship(s) (Supplementary Materials).

The inputs for the decompaction and backstripping portion of SubsidenceChron.jl (Zhang et al., 2023) consist of stratigraphic data and age constraints from the target succession. Stratigraphic inputs, which include units (of variable scales from beds to formations to groups), and their respective lithologies and thicknesses, should ideally start at the beginning of thermal subsidence within the examined basin. The rift-thermal subsidence transition should be identified (or at least reasonably hypothesized) in the studied succession based on a change from active rift-related deposits to passive margin strata (e.g., Meng et al., 2011; Williams and Hiscott, 1987; Yonkee et al., 2014). Decompaction and backstripping procedures typically utilize lithology-dependent parameters for surface porosity, porosity-depth coefficients, and grain density. In traditional basin analysis studies, these parameters are intro-

duced to subsidence models as single values. This poses a problem because the values for these parameters can vary (in some cases, significantly) due to differences in lithologic composition and compaction mechanisms, especially in heterolithic successions. We tackle this issue by first summarizing the distributions of these parameters from published measurements and empirical data (Table 1). Then, we use direct Monte Carlo error propagation wherein a set of values for all parameters with uncertainties is randomly drawn from their respective Gaussian distributions at the beginning of each simulation. The decompacted and backstripped thicknesses calculated from each simulation, representing how tectonic subsidence increases throughout the target succession, are stored in the program as outputs, with summary statistics (means and standard deviations) calculated after all simulations are completed. The summary statistics of these results, along with age-constraint data that are also imported into our model as distributions (see below), are propagated to the next part of the program as inputs to the age-depth model. As part of the backstripping procedure, our model can also incorporate paleo-water depths as distributions and correct for the water-loading effect on subsidence.

2.1.2. Thermal subsidence

The rest of the SubsidenceChron.jl (Zhang et al., 2023) program builds upon the stratigraphic model of Chron.jl (Keller, 2018), which is a Bayesian age-depth model. It uses an MCMC method via the Metropolis algorithm to generate age estimations with uncertainties throughout a given stratigraphic succession while only assuming stratigraphic superposition. Unlike a few other Bayesian age-depth modeling programs, Chron.jl does not force or assume the change in sedimentation rate to be smooth. In this way, it is more similar to Bchron (e.g., Haslett and Parnell, 2008) than to Bacon or OxCal (e.g., Blaauw and Christen, 2011; Ramsey, 2008). However, Chron.jl is different from Bchron in that it models sedimentation as a sequence of individual geologically instantaneous events (Keller, 2018). This is similar to the approach used by Johnstone et al. (2019), but in contrast with Bchron's linear segment-wise treatment, which implicitly requires that sedimentation rate is at least locally (piecewise) constant. The main modification made to the stratigraphic model in Chron.jl by SubsidenceChron.jl is the additional assumption that the amount of tectonic subsidence produced in post-rift sedimentary basins should exponentially decrease through time (McKenzie, 1978). This assumption is manifested in the model as an extra likelihood term, which examines how closely the proposed age-depth curve in each simulation resembles the age-depth relationship predicted by McKenzie (1978). In addition, another likelihood term is added to evaluate each combination of the proposed stretching factor (β) and thermal subsidence initiation time (t_0), which are the two parameters that control the shape of the post-rifting age-depth curve under McKenzie's (1978) framework. The SubsidenceChron.jl package, therefore, is tailored to sedimentary strata that were deposited in thermally subsiding extensional basins.

2.1.3. Performance tests and sensitivity analyses

To evaluate the ability of our method to recover a hypothetical rift scenario, we constructed a synthetic stratigraphic section that was deposited in a McKenzie-style thermally subsiding basin with $\beta = 1.85$ and $t_0 = 400$ Ma. From the synthetic present-day stratigraphy (Fig. 2), the amount of tectonic subsidence produced during the development of this post-rift basin is back-calculated through decompaction and backstripping, without introducing any lithology-dependent errors. Then, we determined the tectonic subsidence versus age relationship based on McKenzie's (1978) thermal subsidence model. We applied this age model to the synthetic stratigraphic section to extrapolate the "real" ages throughout this succession at 20 m resolution.

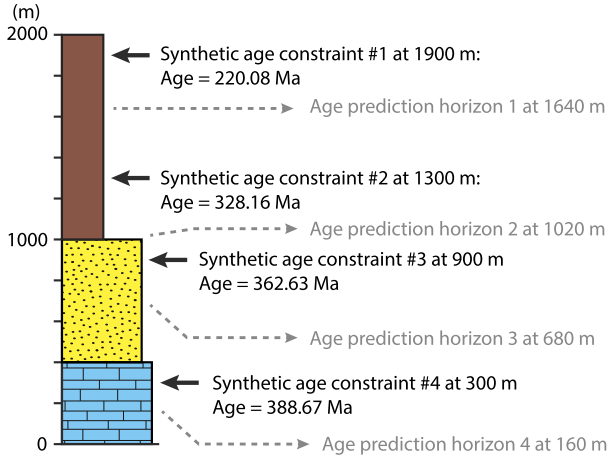

Fig. 2. Stratigraphic column for the synthetic succession, along with horizons for age constraints and age predictions used in the performance tests and sensitivity analyses. Legend for this stratigraphic column is the same as the legend for Fig. 4A.

The performance of the model is first tested by assigning the normal distribution means of the priors β and t_0 to be their true values (with arbitrarily chosen prior standard deviations). We ran the thermal subsidence portion of the SubsidenceChron.jl program using the "real" ages of four randomly selected horizons from our synthetic stratigraphy (Fig. 2). Results show that the true values of both β and t_0 lie within one standard deviation from the posterior means (Fig. 1). Compared with the priors, the posterior standard deviations are significantly smaller, which agrees with our expectation. In addition, we tested the ability of our model to accurately predict ages for previously undated horizons. The age predictions, also in the form of distributions, were calculated using β and t_0 values that fall within the 95% credible intervals of their respective posterior distributions. For all four randomly picked horizons, our model was able to generate age distributions that are almost centered on the synthetic "real" ages, with all predicted medians lying within ~3 Ma from the true values (Fig. 3).

We then examined the robustness of the model by reshaping the prior distributions of the two parameters. For each test, we only adjusted one attribute of the prior distribution (either mean or standard deviation) for one of the subsidence parameters (either β or t_0) while keeping the rest of the inputs constant. The posterior distributions all converged towards the real values of β and t_0 (Fig. 3), indicating that our model does not heavily depend on the prior distributions. Although the posterior standard deviation for t_0 (particularly the extent of the upper tail) is somewhat sensitive to changes in the prior, the true values of the subsidence parameters still fell within one standard deviation of the posterior mean in all tests (Fig. 2).

2.2. Re-Os and U-Pb geochronology

We present a new Re-Os age from organic-rich mudstone in the Svanbergfjellet Formation collected in Lomfjorden, Ny Friesland (Figs. 4 and 5). Our sample (J1643) was collected 1.1 m below the first major stromatolite buildup marking the base of the upper Algal member of the Svanbergfjellet Formation. Detailed information on sample preparation and Re-Os isotopic analyses are presented in the Supplemental Materials.

We also present new U-Pb data from detrital zircons collected from a bed of medium-grained calcareous quartz arenite in the Bogen Member of the Kingbreen Formation, Veteranen Group (sample J1635). This sample was collected ~2.2 km below the base of the Akademikerbreen Group in Fakesevågen, Ny Friesland (Fig. 4;

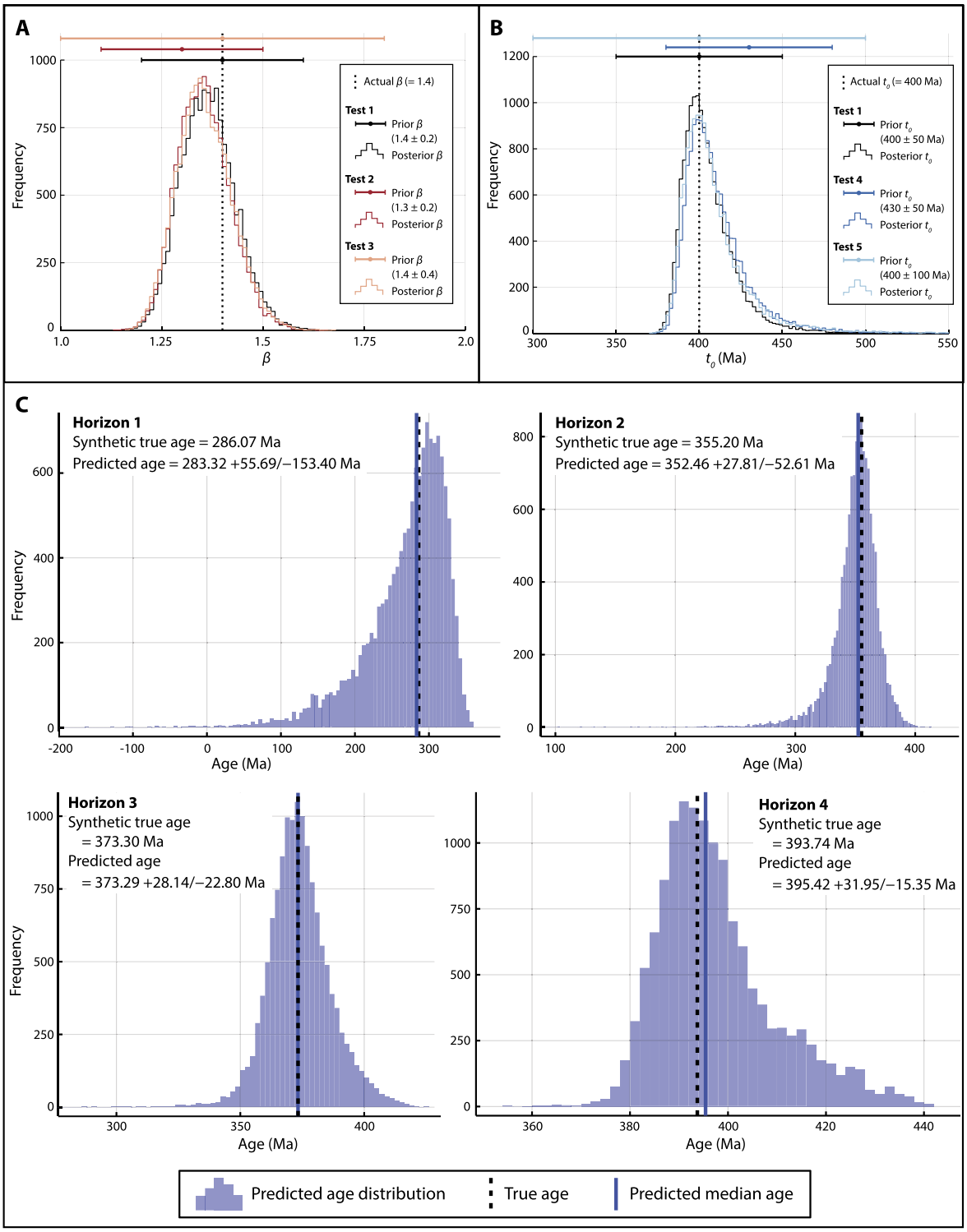

Fig. 3. Results from sensitivity analyses on a synthetic sedimentary succession using SubsidenceChron.jl showing the effects of prior perturbations on the posterior distributions. (A) Posterior distributions of β generated from various prior conditions of β, showing that the posterior successfully converged around its true value despite perturbations in the prior. (B) Posterior distributions of t_0 generated from various conditions of t_0, also suggesting that perturbations in the prior do not affect the model's ability to successfully produce accurate posterior distributions. (C) Age predictions for randomly selected horizons at 160, 680, 1020, and 1640 m in the synthetic stratigraphic section, compared with the synthetic true ages of these horizons.

Gibson et al., 2021). Zircons from sample J1635 were first analyzed by laser ablation-inductively coupled mass spectrometry (LA-ICPMS). The seven youngest detrital zircon grains were then analyzed by chemical abrasion-thermal ionization mass spectrometry (CA-TIMS) to provide a high-precision maximum depositional age for these strata. Detailed descriptions of the sample preparation and analytical methods are described in the Supplementary Materials.

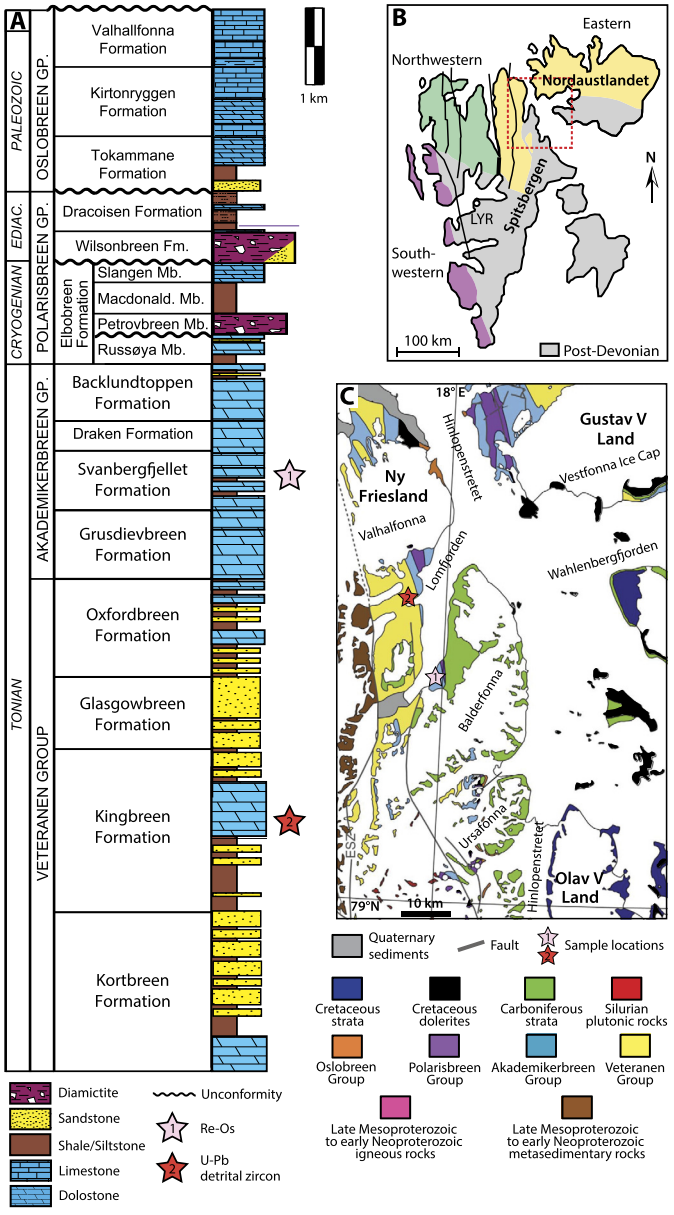

Fig. 4. Geologic background for the case study. (A) Generalized Neoproterozoic to Ordovician stratigraphy of northeastern Svalbard showing the stratigraphic positions of the new radiometric age constraints provided herein. EDIAC. – Ediacaran; GP. – Group; Fm. – Formation; Mb. – Member. Modified after Gibson et al. (2021). (B) Simplified geologic map of Svalbard showing the location of Fig. 2C (red dashed box). Basement domains and major faults are indicated and modified after Halverson et al. (2018a) LYR – Longyearbyen. (C) Geologic map of northeastern Svalbard showing the sampling locations for the new geochronologic constraints after Hoffman et al. (2012) ESZ – Eolusletta Shear Zone.

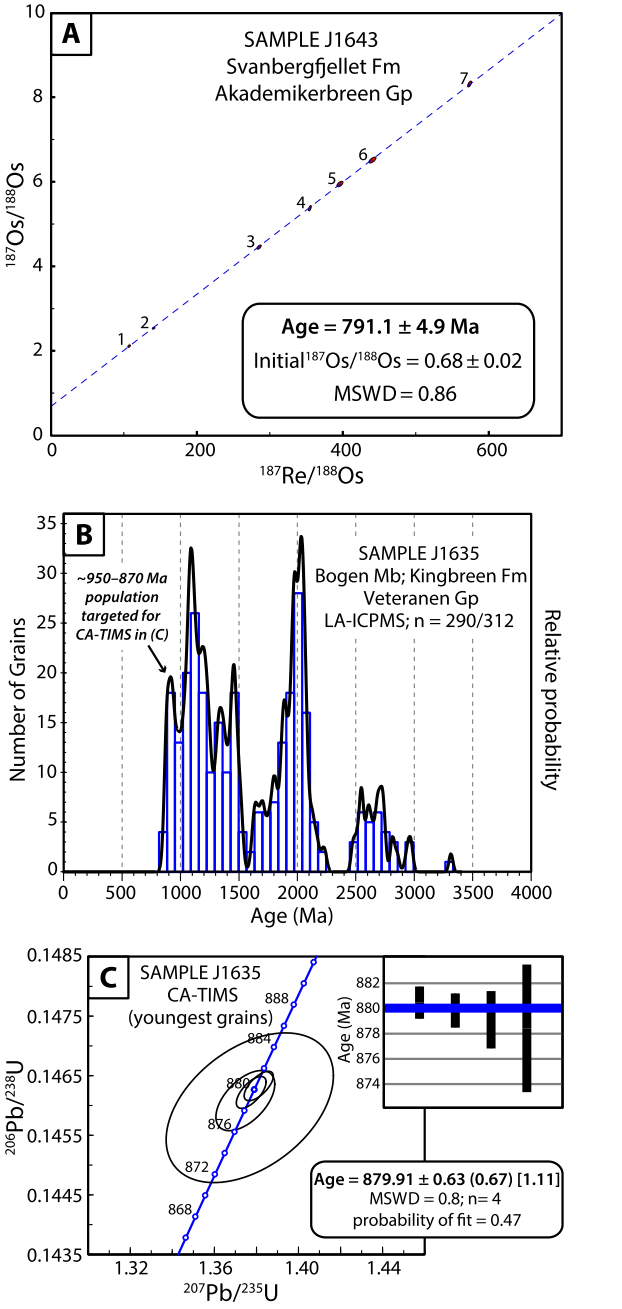

Fig. 5. New geochronological constraints on the Veteranen and Akademikerbreen groups of northeastern Svalbard. A) Re-Os isochron diagram of sample J1643 from the Svanbergfjellet Formation. Data point labels correspond to those in Table S1 (see Supplemental Materials), and the data point ellipses represent 2σ uncertainty and include the uncertainty of the ^{187}Re decay constant; MSWD – mean square of weighted deviates. B) Histogram and probability density plot of detrital zircon U-Pb isotopic results from sample J1635 of the Bogen Member of the Kingbreen Formation (Veteranen Group). The youngest grains from this sample were analyzed by CA-TIMS. C) Concordia diagram and weighted mean (inset) plots of U-Pb CA-TIMS isotopic results from the four youngest detrital zircon grains in sample J1635 shown in B). The ellipses and weighted mean bars represent 2σ uncertainty.

3. Case study: Tonian Veteranen and Akademikerbreen Groups, Svalbard, Norway

3.1. Geologic background

The Svalbard archipelago of Norway consists of three pre-Devonian basement provinces that are separated by north-south-trending strike-slip fault zones (Harland, 1997). The Eastern basement province, which is exposed on northeastern Spitsbergen and Nordaustlandet (Fig. 4), hosts a package of well-preserved Neoproterozoic-Ordovician sedimentary strata known as the Hecla Hoek succession (Flood et al., 1969; Kulling, 1934; Sandford, 1926). The basal ~4 km-thick Veteranen Group unconformably overlies Stenian–Tonian metasedimentary and volcanic rocks on Nordaustlandet and is mainly comprised of siliciclastic strata with minor carbonate intervals (Gibson et al., 2021; Sandelin et al., 2001, and references therein). These strata have a ca. 940 Ma maximum depositional age (Gibson et al., 2021; Sandelin et al., 2001) and transition upwards into the ~2 km-thick carbonate-dominated middle to late Tonian Akademikerbreen Group. The Akademikerbreen Group (Grusdievbreen, Svanbergfjellet, Draken and Backlundtop-

pen formations) has no published radiometric dates, but it does record the ca. 810–788 Ma Bitter Springs negative carbon isotope excursion (CIE) (Cohen et al., 2017; Halverson et al., 2005, 2018a; Macdonald et al., 2010; Swanson-Hysell et al., 2012, 2015). These strata are overlain by the late Tonian to early Ediacaran Polarisbreen Group, which is comprised of mixed siliciclastic and carbonate strata of the Elbobreen, Wilsonbreen, and Dracoisen formations. Glacial deposits of the Sturtian and Marinoan snowball Earth events, both with unconformable basal contacts, are recorded in the lower-middle Polarisbreen Group (Hoffman et al., 2012). The Ediacaran portion of the Hecla Hoek succession is unconformably overlain by the carbonate-dominated Cambrian–Ordovician Oslobreen Group (Fortey and Bruton, 1973; Gobbett and Wilson, 1960; Harland and Wilson, 1956).

Most paleogeographic reconstructions have placed the Eastern basement province of Svalbard along the northeastern margin of Laurentia during the Tonian (e.g., Harland, 1997; Hoffman et al., 2012; Maloof et al., 2006). The lower Hecla Hoek series presumably records a transition from contraction and arc magmatism (e.g., Gee et al., 1995; Johansson et al., 2005) to active rifting, which is most likely represented by the Veteranen Group (Gibson et al., 2021), to passive margin sedimentation in the Akademikerbreen Group (e.g., Maloof et al., 2006). The recent subsidence model of Halverson et al. (2022) suggested an 816.8 ± 3.6 Ma age for the timing of this rift-drift transition. Since our subsidence model is only designed for reconstructing the age-depth relationship during thermal subsidence, stratigraphic input data are focused on the Akademikerbreen Group and the sub-Sturtian Russøya Member of the Elbobreen Formation (Fig. 4). Furthermore, to avoid any presumed age biases for the reconstruction of our age-depth relationships, we do not consider any correlated age constraints provided by chemostratigraphic correlations from other Tonian successions (e.g., Halverson et al., 2018b, 2022).

3.2. New age constraints and subsidence model age parameters

Re-Os geochronological analyses on sample J1643 from the Svanbergfjellet Formation yielded a Model 1 age of 791.1 ± 4.9 Ma (n = 7, mean square of weighted deviation, MSWD = 0.86) with an initial $^{187}Os/^{188}Os$ (Os_i) composition of 0.68 ± 0.02 (Fig. 5A; Table S1). Total uncertainties are reported at 2σ and include the uncertainty associated with the ^{187}Re decay constant (Smoliar et al., 1996). This represents the first published radiometric age constraint from the Akademikerbreen Group.

In addition to this new depositional age within the Svanbergfjellet Formation, we also utilize another recently published radiometric age from the upper Russøya Member of the Elbobreen Formation, which is a Re-Os age of 737.5 ± 9.6 Ma (Millikin et al., 2022). Furthermore, because the synchroneity for the initiation of the Sturtian snowball Earth event has been well established (e.g., Macdonald et al., 2010; MacLennan et al., 2018; Pu et al., 2022), we include the onset of the Sturtian glaciation as a one-sided (minimum) age constraint at 717 +0.7/−0.9 Ma. The stratigraphic position of this constraint is placed at the Russøya-Petrovbreen contact (Fig. 4), immediately above an unconformity of unknown duration. To avoid complications caused by the unknown amount of erosion at the base of the Petrovbreen Member, our subsidence model only outputs age-depth relationships through the upper Russøya Member of the Elbobreen Formation.

U-Pb CA-TIMS analyses on detrital zircons from sample J1635 provide a one-sided maximum depositional age on the Akademikerbreen Group. The four youngest dates yield a weighted mean of 879.91 ± 0.63/0.67/1.11 Ma (MSWD = 0.8, probability of fit = 0.47; Fig. 5B; Table S4); errors are given as ± x/y/z, where x is the internal error based on analytical uncertainties only, including counting statistics, subtraction of tracer solution, and blank and initial common Pb subtraction, y includes the tracer calibration uncertainty propagated in quadrature, and z includes the ^{238}U decay constant uncertainty propagated in quadrature. The three other detrital zircons yielded older individual U/Pb dates of 1680.97 ± 5.84, 906.45 ± 0.95, and 901.85 ± 0.67 Ma.

3.3. Subsidence modeling results

We first ran the decompaction and backstripping portion of the SubsidenceChron.jl (Zhang et al., 2023) program for 5000 Monte Carlo simulations at 1 m resolution. The lithology-dependent parameter inputs, as well as water depth distributions for different depositional environments, are listed in Table 1. The lithostratigraphic inputs for the Svalbard succession are extracted from the composite section in Halverson et al. (2018a). Water depth predictions are obtained from the sedimentological and paleoenvironmental analyses in Halverson et al. (2007, 2018a), which document that this succession was predominantly deposited in a shallow marine setting above storm wave base. Our modeling results show that the input uncertainties have been successfully propagated to the model outputs, which are manifested as standard deviations up to ∼72 m on the tectonic subsidence curves (Fig. 6A).

These results, along with the new and published age constraints presented in the previous section, are used as inputs in the thermal subsidence age-depth modeling portion of the SubsidenceChron.jl (Zhang et al., 2023) program. All age inputs are assigned with a stratigraphic height uncertainty of 10 m to account for the height discrepancies between the composite section and the sections from which the geochronologic constraints were sampled. The prior means for β and t_0 are set equal to their posterior means presented by Halverson et al. (2022), which are 1.3 and 816 Ma, respectively. As demonstrated in section 2.1.3, however, the choice of prior distribution is nonunique as long as it captures the broad framing of the scenario (i.e., as long as the 95% credible interval of the prior distributions of β and t_0 encapsulate their true values). We ran the MCMC model for 10,000 steps after 1.4 x 10^7 iterations of burn-in (i.e., running the model but discarding the results) to ensure that equilibrium distribution was reached. From the base of the Akademikerbreen Group to the onset of the Sturtian glaciation, our model outputs a posterior β = 1.29+0.08/−0.06 and a posterior t_0 = 840.40+18.64/−23.61 Ma (Fig. 6C-D; results are reported as medians and 95% credible intervals). For key stratigraphic boundaries, namely 1) the base of Draken Formation, 2) the base of Russøya Member of the Elbobreen Formation, and 3) the top of the Russøya Member, the age predictions are 1) 783.97+7.39/−10.93 Ma, 2) 739.09+9.53/−9.54 Ma, and 3) 728.57+10.59/−10.02 Ma.

4. Discussion

4.1. Case study: implications for the Tonian of Svalbard

4.1.1. Comparison with previous subsidence models

Like the approach of Halverson et al. (2018b, 2022), the core design of our model is to establish the age-depth relationship of a given sedimentary succession using a Bayesian framework for subsidence analysis. However, there are several significant differences in the implementation and execution of our model with respect to the previous work of Halverson et al. (2018b, 2022). First, our model incorporates decompaction and backstripping procedures, which were not considered by Halverson et al. (2022). Although the effect of these procedures is less pronounced in the lower part of the Tonian succession in Svalbard where one lithology tends to dominate, they become important when estimating the amount of tectonic subsidence in the lithologically diverse and shale-dominated upper part of the succession. Through

Table 1
Model parameters. Distributions for lithology-dependent parameters are compiled from Sclater and Christie (1980), Hölzel et al. (2008), and Giles et al. (1998). Distributions for the facies-dependent parameter (paleo-water depth) are obtained from Allaby (2008). Values for other parameters are obtained from Allen and Allen (2013). The N(X, Y) notation represents a normal distribution with a mean of X and a standard deviation of Y. The U(A, B) notation represents a uniform distribution over the interval [A, B]. FWWB – Fair weather wave base; SWB – Storm wave base.

Lithology-dependent parameters	Unit	Type	Data
Surface porosity (ϕ_0)	N/A	Shale	N(0.63, 0.15); truncated at 0 and 1
		Sandstone	N(0.49, 0.1); truncated at 0 and 1
		Dolostone	N(0.2, 0.1); truncated at 0 and 1
		Limestone	N(0.4, 0.17); truncated at 0 and 1
Porosity-depth coefficient (c)	km-1	Shale	N(0.51, 0.1); truncated at 0
		Sandstone	N(0.27, 0.06); truncated at 0
		Dolostone	N(0.6, 0.2); truncated at 0
		Limestone	N(0.6, 0.2); truncated at 0
Grain density (ρ_g)	kg^*m^{-3}	Shale	2720
		Sandstone	2650
		Dolostone	2870
		Limestone	2710
Facies-dependent parameter	**Unit**	**Type**	**Data**
Paleo-water depth (W_d)	m	Exposure	U(0, 0.01)
		Above FWWB	U(5, 15)
		FWWB-SWB	U(15, 40)
Other parameters			**Data with unit**
Water density (ρ_w)			1000 kg^*m^{-3}
Mantle density at 0 °C (ρ_m)			3330 kg^*m^{-3}
Lithospheric thickness (y_L)			125000 m
Volumetric coefficient of thermal expansion (α_v)			3.28^*10^{-5} $°C^{-1}$
Temperature of asthenosphere (T_m)			1333 °C
Thermal time constant (τ)			50 Myr

the utilization of decompaction and backstripping techniques, we are also able to introduce lithology-related uncertainties into the model, which are commonly absent in most basin analysis studies (see below). Second, the two models treat the theoretical thermal subsidence age-depth relationship differently. While Halverson et al. (2022) assume that the age-depth curve for every simulation perfectly follows the theoretically derived relationship (Eq. S3), our model does not force this shape onto the model outputs (Fig. 6B). Instead, SubsidenceChron.jl (Zhang et al., 2023) only uses this relationship as one of the criteria to evaluate individual MCMC candidates. Finally, as stated above, our model only accepts radiometric ages from the Svalbard succession alone as inputs, whereas Halverson et al. (2018b, 2022) rely on correlated ages from global chemostratigraphic datasets. Thus, our model makes fewer assumptions about the correlated age constraints of an individual succession and avoids potential errors associated with local diagenetic overprints, issues of condensation or subtle disconformities, or inaccurate chemostratigraphic correlations. One caveat in our model design is that the stratigraphic position of the rift-drift transition needs to be identified prior to running the model and cannot be evaluated in the MCMC calculations; this can be achieved by Halverson et al. (2022)'s model, so in theory the two approaches could be used simultaneously to explore the full parameter space of an individual sedimentary succession.

To make meaningful comparisons, we reran the Halverson et al. (2022) model with the new Re-Os from the Svanbergfjellet Formation, which resulted in minor changes to the model outputs. The differences in these two approaches translate to a few notable deviations in the results of the age-depth relationships for the Tonian strata of northeastern Svalbard. First, the uncertainties on all our model outputs are larger than those from the Halverson et al. (2022) model (Figs. 6C-D and 7). The 95% credible intervals on the posterior β and t_0 from our model are approximately six to seven times larger than those from the Halverson et al. (2022) model, and the individual formation boundary age predictions of our model are generally two to three times larger (Fig. 7D, E and G). For example, the Halverson et al. (2022) model, after rerunning with the new Re-Os age, reported a 95% credible interval of $+3.52/-3.59$ Ma for t_0, whereas our model returned $+18.64/-23.61$ Ma for the same variable. As for the onset of the Russøya CIE, the 95% credible interval from Halverson et al.'s (2022) model is $+4.57/-4.96$ Ma, whereas we report an uncertainty of $+9.51/-9.67$ Ma. The larger uncertainties on our posteriors and model predictions are the results of: 1) the additional input uncertainties incorporated into our model (e.g., subsidence parameters, decompaction, and paleo-water depth predictions); and 2) the smaller number of available age constraints (four versus eleven). Both factors reflect legitimate geological complexities that must be grappled with when trying to generate accurate age-depth models using a subsidence analysis approach, and the larger uncertainties from our model are more direct representations of the known Tonian age-depth relationships in northeastern Svalbard. Second, our calculated prediction for the onset of thermal subsidence at the Veteranen–Akademikerbreen Group boundary leans towards the older side of the distribution presented in Halverson et al. (2022). Although there is some overlap between the two posterior distributions for t_0, the posterior mean t_0 from Halverson et al. (2022) is located near the upper bound of the 95% credible interval for the posterior t_0 of our study (Fig. 6D). This may be a function of an artificially steep subsidence gradient at the onset of Halverson et al.'s (2022) rift-drift transition, or the use of modern-day stratigraphic heights instead of heights corrected for decompaction and tectonic subsidence. This discrepancy is important as it exerts a strong control on the total amount of subsidence that the Tonian rifting event can ultimately generate.

4.1.2. Testing the validity of Neoproterozoic global chemostratigraphic correlation

The employment of carbon isotope chemostratigraphy for global correlations of Proterozoic sedimentary successions was first docu-

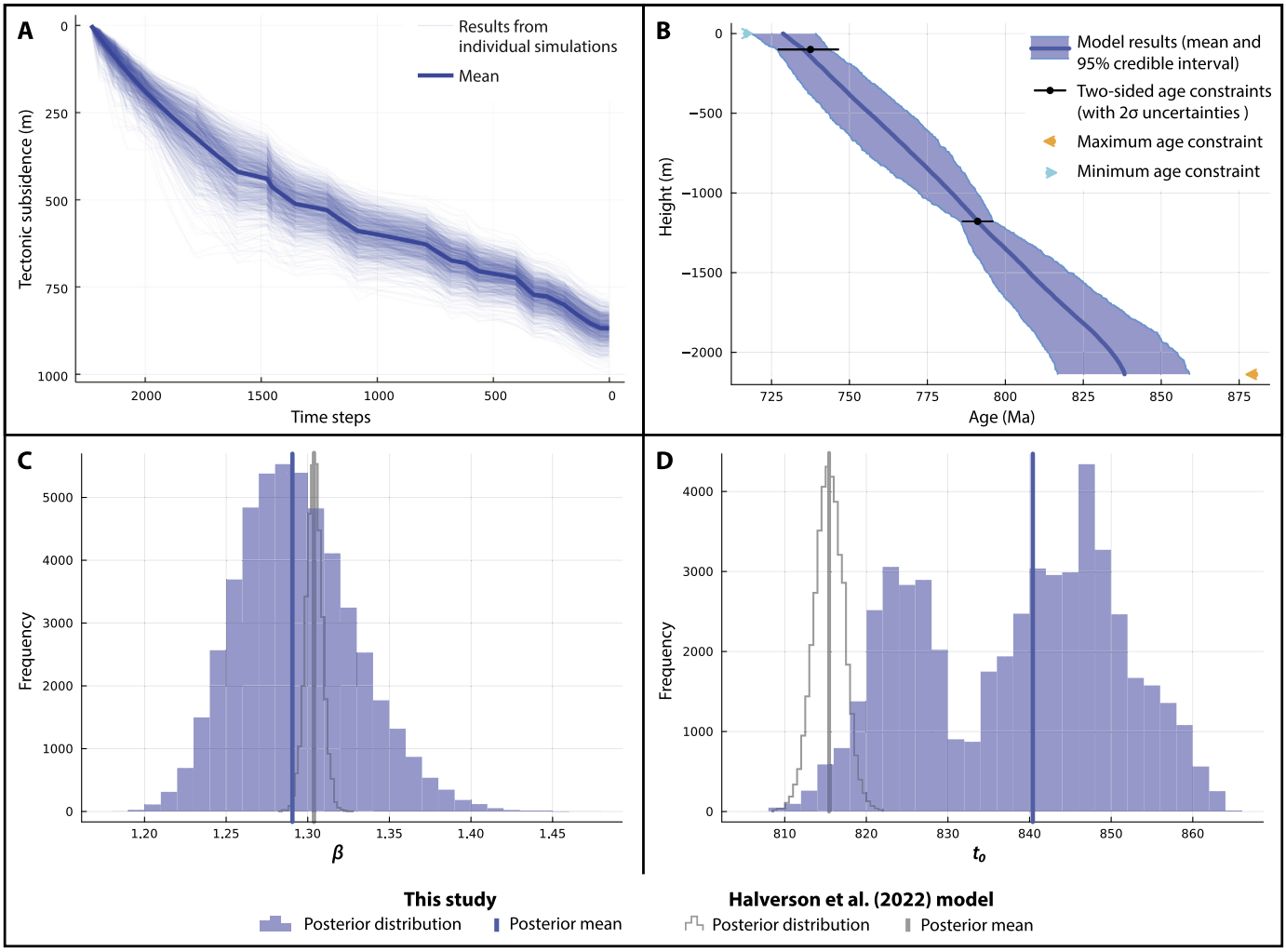

Fig. 6. Model results for the northeastern Svalbard Tonian case study. (A) Outputs from the decompaction and backstripping portion of the program showing tectonic subsidence from 1000 individual Monte Carlo simulations, as well as the summary statistics (mean). (B) Age-depth model with uncertainties for the northeastern Svalbard succession. Age constraints with uncertainties are also plotted. (C) Posterior distribution for the stretching factor β, compared with the posterior of β from the Halverson et al. (2022) model. (D) Posterior distribution for the age of thermal subsidence initiation t_0, compared with the posterior t_0 from the Halverson et al. (2022) model. See text for further explanation.

mented by Knoll et al. (1986) on this same succession in Svalbard, and it has since served as one of the most widely used tools to correlate Precambrian strata worldwide (e.g., Halverson et al., 2005; Macdonald et al., 2010; Shields et al., 2021). The Tonian succession in the Eastern basement province of Svalbard records two pronounced and globally identifiable negative CIEs. The older Bitter Springs CIE occurs in the upper Grusdievbreen and lower Svanbergfjellet formations of the Akademikerbreen Group (Fig. 7A), and it is characterized by a prolonged $\delta^{13}C_{carb}$ perturbation down to $\sim -4‰$ from a background state of $\sim 5‰$. Although there are no radiometric age constraints for the Bitter Springs CIE in Svalbard, the onset of this event has been constrained by a zircon U-Pb CA-TIMS age of 811.51 ± 0.25 Ma from a tuff horizon immediately preceding the CIE in the Fifteenmile Group of the Ogilvie Mountains in Yukon, Canada (Macdonald et al., 2010). In the western Ogilvie Mountains along the U.S.-Yukon border, a Re-Os age of 810.7 ± 6.3 Ma from a black shale horizon in roughly the same stratigraphic position also provides a maximum age constraint on the Bitter Springs CIE (Cohen et al., 2017). The global synchroneity of this CIE is supported by a U-Pb CA-TIMS zircon age of 815.29 ± 0.32 Ma from a tuff horizon predating the excursion in the Werri Formation of the Tambien Group in Ethiopia (Swanson-Hysell et al., 2015). The Tambien Group also yielded U-Pb zircon ages of 788.72 ± 0.24 Ma and 787.38 ± 0.14 Ma from tuff beds in the upper Tsedia Formation that postdate the Bitter Springs CIE (MacLennan et al., 2018; Swanson-Hysell et al., 2015).

The younger Russøya CIE is recorded in the upper Russøya Member of the Elbobreen Formation (Polarisbreen Group) in Svalbard. Locally this excursion reaches a minimum $\delta^{13}C_{carb}$ value of $\sim -7‰$ and a partial recovery to less depleted ratios prior to its truncation beneath Sturtian glacial deposits of the overlying Petrovbreen Member. As highlighted above, a Re-Os date of 737.5 ± 9.6 Ma was recently published by Millikin et al. (2022) from 44 m below the initiation of the Russøya CIE in Nordaustlandet. This is in general agreement with a Re-Os age of 739.9 ± 6.5 Ma for the nadir of the Russøya CIE in the Callison Lake Formation of the Ogilvie Mountains (Strauss et al., 2014). In the Mackenzie Mountains of Northwest Territories, Canada, the recovery from the nadir of the Russøya CIE occurs within the Coppercap Formation of the Coates Lake Group, which was dated to 732.2 ± 4.7 Ma using Re-Os geochronology (Rooney et al., 2014). The nadir of this CIE was also constrained in Ethiopia, where a volcanic tuff horizon in the upper Tambien Group yielded a U-Pb CA-TIMS zircon age of 735.25 +0.25/−0.88 Ma (MacLennan et al., 2018).

Since our subsidence age-depth model for the Tonian succession of northeastern Svalbard only uses local age constraints as

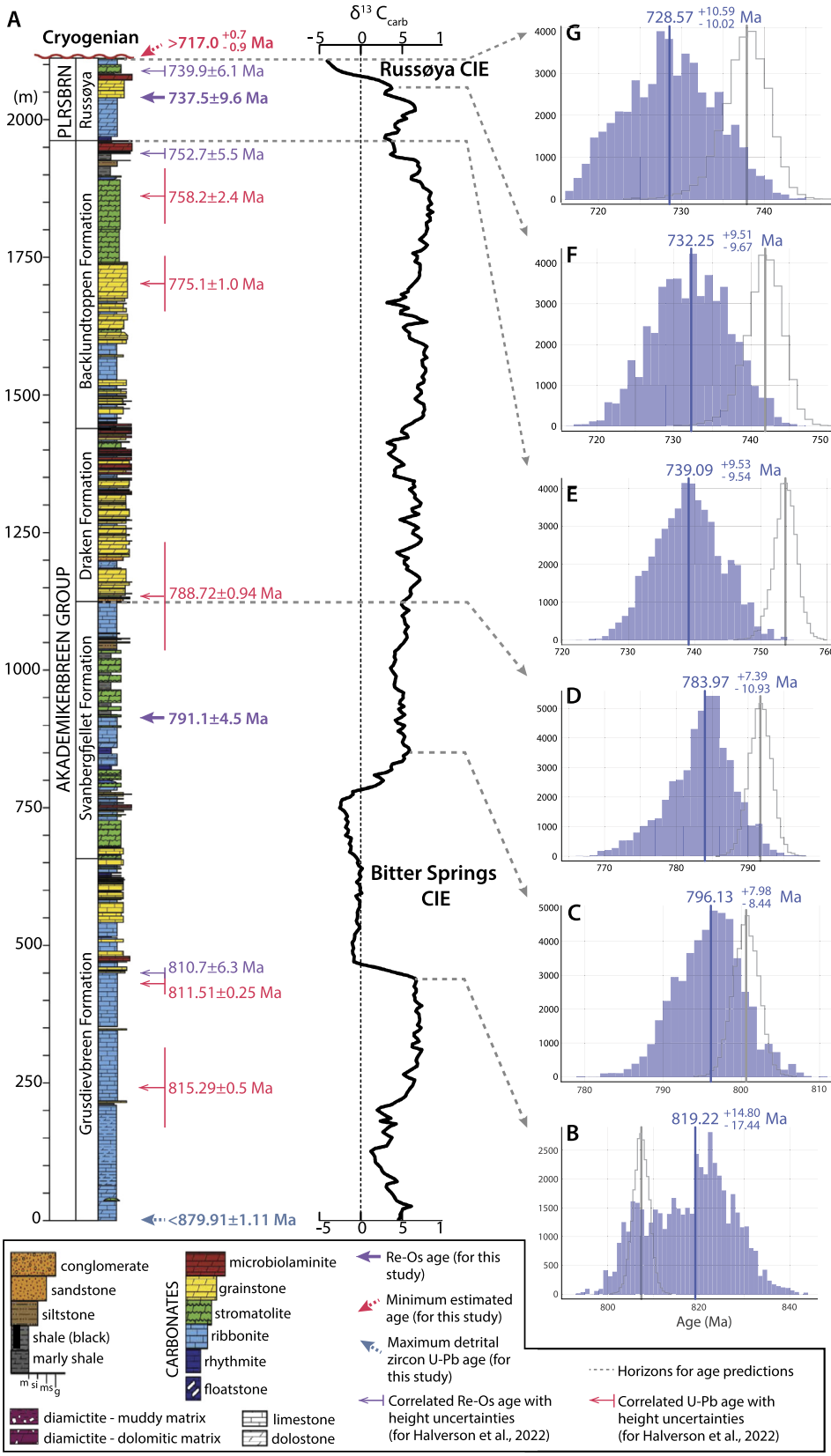

Fig. 7. Age predictions for the northeastern Svalbard Tonian case study in the context of litho- and chemostratigraphic data. (A) Composite stratigraphic column for the Tonian strata of northeastern Svalbard along with the composite carbon isotope $\delta^{13}C$ curve and stratigraphic locations of local geochronologic constraints, correlated geochronologic constraints, and age predictions. Modified after Halverson et al. (2018a). PLRSBRN – Polarisbreen Group; Russøya – Russøya Member. Age predictions from SubsidenceChron.jl are plotted in blue against the age estimations from the Halverson et al. (2022) model in grey for the following formation boundaries and horizons of chemostratigraphic significance: (B) the onset of Bitter Springs CIE, (C) the termination of Bitter Springs CIE, (D) the base of the Draken Formation, (E) the base of the Elbobreen Formation, (F) the onset of the Russøya CIE, and (G) the top of the Russøya Member of the Elbobreen Formation. Legend for Fig. 5B–G is the same as the legend for Fig. 6C-D.

inputs, it can serve as an independent test of the validity of predicted carbon isotope chemostratigraphic correlations. Based on our age-depth model, the predicted 95% credible interval for the onset of the Bitter Springs CIE is 819.22 +14.80/−17.44 Ma (Fig. 7B), while the predicted age for the termination of the CIE is 796.13 +7.98/−8.44 Ma (Fig. 7C). For the Russøya CIE, our model has an onset age estimation of 732.25+9.51/−9.67 Ma (Fig. 7F). All three model-predicted age distributions from the Svalbard section overlap with the radiometric age constraints on the respective CIEs from other successions (Fig. 7B, C, and F), which broadly supports the hypothesis that these CIEs are likely contemporaneous across multiple globally distributed basins. However, due to the large credible intervals on the age predictions, it is insufficient to argue unambiguously about their global synchroneity. Despite this, the large uncertainty envelopes are expected since the Tonian succession in Svalbard only hosts a small number of radiometric age constraints, some of which are ∼500 m above or below the closest horizon of interest. If more age constraints are discovered in the future, our approach will be able to output more precise age predictions and further refine the Tonian chemostratigraphic framework of Svalbard.

4.1.3. Implications for the Neoproterozoic–early Paleozoic tectonic evolution of Svalbard

The boundary between the Ediacaran Polarisbreen and Cambrian–Ordovician Oslobreen groups has long been identified as a significant disconformity in northeastern Svalbard (e.g., Harland, 1997; Knoll and Swett, 1987, and references therein). Several researchers have hypothesized that this unconformity is associated with a renewed phase of rifting in the Eastern basement province of Svalbard (e.g., Harland, 1997; Herrington and Fairchild, 1989; Maloof et al., 2006). However, this hypothesis remains speculative since no Ediacaran–Cambrian rift-related volcanic rocks or other sedimentological evidence for extension have been reported. To test this hypothesis, we utilized our subsidence model to investigate whether the Tonian rift event that apparently ceased at the base of the Akademikerbreen Group was responsible for generating the accommodation space needed to host the overlying Polarisbreen and Oslobreen groups.

First, we employed the rift conditions (β and t_0) generated from the SubsidenceChron.jl (Zhang et al., 2023) model to estimate the cumulative amounts of tectonic subsidence that can be generated (i.e., "predicted tectonic subsidence") for a few younger horizons of interest. Meanwhile, we extended our decompaction and backstripping procedures into the younger part of the succession and calculated the amount of tectonic subsidence that is needed to host these overlying strata (i.e., "required tectonic subsidence"). The comparison between these two approaches suggests that the Tonian rift event, which accommodated the Akademikerbreen and lower Polarisbreen groups during its thermal subsidence phase, cannot account for the total amount of basin subsidence needed to explain the thicknesses of the upper Polarisbreen and Oslobreen groups (Fig. 8). For example, using a horizon in the Dracoisen Formation ∼600 m above the top of the Russøya Member that was recently dated with Re-Os geochronology to 631.2 ± 3.8 Ma (Millikin et al., 2022), we found the required tectonic subsidence is >200 m more than the mean tectonic subsidence supplied in the Tonian rift event. The second horizon, for which we chose the Ediacaran-Cambrian transition at the top of the Dracoisen Formation, yielded a mean predicted tectonic subsidence of ∼891 m. The mean required tectonic subsidence, however, is ∼1315 m. In other words, sediment deposited between these two horizons requires an additional ∼231 m of accommodation space, which is an order of magnitude larger than the 13 m of thermal subsidence that the initial Tonian rift event can generate.

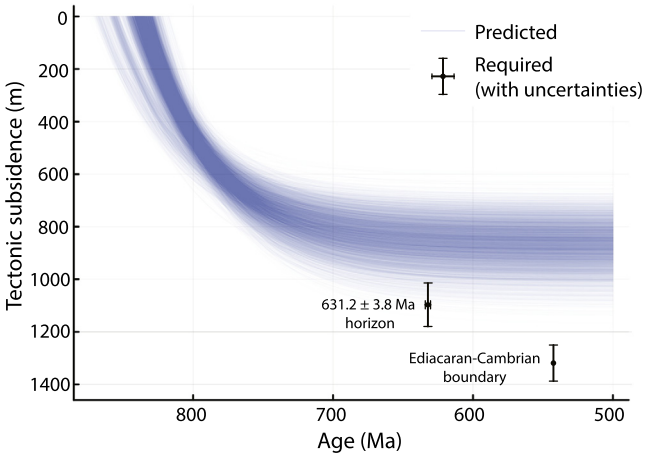

Fig. 8. Basin evolution of northeastern Svalbard post-dating the Tonian Period. Required tectonic subsidence for 1) the 631.2 ± 3.8 Ma horizon and 2) the Ediacaran-Cambrian transition plotted against the predicted tectonic subsidence (based on the posterior β and t_0) following the Tonian rifting event for the Svalbard succession.

These discrepancies suggest that the Tonian extension cannot generate enough subsidence to accommodate the upper Polarisbreen and Oslobreen groups in Svalbard. Thus, other mechanisms, likely renewed extension, must be invoked to generate the necessary accommodation space for the carbonate-dominated Oslobreen Group. The possible timing for this second phase of rifting is speculative due to the dearth of rift-related deposits or volcanic rocks, but it is likely either syn-Russøya or somewhere within the Polarisbreen–Oslobreen group unconformity (e.g., Harland, 1997; Halverson et al., 2018a). Although there is no evidence to rule out episodic extensions throughout the Polarisbreen Group or some combination of the two likely scenarios, we favor more significant terminal Ediacaran–early Cambrian extension since it is consistent with the broader extensional history of northeastern Laurentia (e.g., Cawood et al., 2001, 2007; Faehnrich et al., in press; Gee and Teben'kov, 2004; Smith and Rasmussen, 2008; Surlyk, 1991; Swett, 1981; Wala et al., 2021).

4.2. Implications for subsidence modeling in Precambrian and Phanerozoic basins

The underlying mathematical model (McKenzie, 1978) for thermally subsiding extensional basins is likely a gross oversimplification of the true extensional history of most rift basins. Factors such as heat flow, mantle flow and dynamic topography, and differences in the physics of lithospheric extension (e.g., instantaneous uniform stretching versus protracted or depth-dependent extension) will all exert significant unquantified controls on the age-depth relationship during thermal subsidence (e.g., Cochran, 1983; Beaumont et al., 1982; Davis and Kusznir, 2004; Huismans and Beaumont, 2014; Jarvis and McKenzie, 1980; Pedersen and Ro, 1992). As a result, future iterations of this approach will need to address these types of potential modifications. Moreover, SubsidenceChron.jl (Zhang et al., 2023) is not yet able to properly model large unconformities with unknown durations (i.e., multi-million-year unconformities that cause regional-scale base level falls, such as large glacio-eustatic fluctuations) within a given sedimentary succession; as a result, unconformity-riddled successions could suffer from an underestimation of the stretching factor β and older age estimations for horizons above the unconformity. Despite these limitations, this study is an important step forward in robustly quantifying uncertainties in basin analysis techniques and it will undoubtedly help with generating future age models for poorly constrained sedimentary successions.

The northeastern Svalbard Tonian succession benefits from abundant and consistent water depth-specific sedimentological data that allow for a relatively strong control on paleo-water depth predictions throughout the modeled composite section. Specifically, according to the paleoenvironmental analyses presented in Halverson et al. (2018a), ~93% of the succession was deposited above storm wave base. However, paleo-water depth predictions may be more ambiguous in other post-rift successions due to insufficient or inconclusive depositional environment indicators. Under such circumstances, future users of SubsidenceChron.jl will need to be cautious in addressing these predictions and to consider increasing the uncertainties accordingly.

Depending on the number and quality of individual radiometric and/or relative age constraints in a given sedimentary succession, the age predictions and other outputs from our modeling approach will unavoidably have larger errors than past versions of thermal subsidence modeling. This is clearly demonstrated by the comparison of our results to those from Halverson et al. (2022) (see section 4.1.1). Although this outcome may be less desirable, it may be more representative of our limited extent of knowledge about an ancient sedimentary basin. Introducing these types of uncertainties into subsidence analysis age-depth modeling is particularly crucial for Precambrian basins, since only a small fraction of their geochronologic and stratigraphic information is obtainable from the present-day rock record.

Despite generally being better characterized and dated, Phanerozoic strata deposited in post-rift basins can also benefit greatly from this new tool. Proper treatment of uncertainties is always desired in quantitative subsidence analyses, regardless of the abundance of geochronological data. Moreover, when more age constraints are inputted into SubsidenceChron.jl, the model yields more precise (i.e., smaller uncertainty envelopes) and geologically meaningful results. Such results could help decipher subtle influences of other geophysical processes beyond the simple McKenzie-type rifting scenario, such as the potential influences of localized heat flow, depth-dependent extension, variable subsidence, volcanic processes, or dynamic topography. Age predictions generated through SubsidenceChron.jl using local radiometric age constraints can also help add uncertainties to biostratigraphic zonation data or first-/last- appearance datums in a given sedimentary succession. Furthermore, similar to many Precambrian successions, some Phanerozoic offshore basins are also poorly constrained due to limited biostratigraphic or radiometric age control, so these successions would be ideal targets for our model. Overall, we suggest that the incorporation and propagation of uncertainties, as demonstrated in this study, are critical for the field of quantitative basin analysis, even in well-characterized and well-dated Phanerozoic basins, since the combination of better-quantified parameters and uncertainty treatments ultimately yields better geological insights (e.g., VanderLeest et al., 2022).

5. Conclusions

We developed a package, SubsidenceChron.jl (Zhang et al., 2023), that can construct age-depth models for sedimentary successions deposited in post-rift thermally subsiding basins. Building upon a McKenzie-style rift model (McKenzie, 1978), the main innovation of our model is the incorporation and propagation of uncertainties in important modeling parameters. In particular, the first part of the model performs decompaction and backstripping calculations to tease out the proportion of basin subsidence caused by tectonic forcings. Uncertainties in lithology-dependent parameters are propagated using Monte Carlo simulations. The second part of our program explores the age-depth relationship in a Bayesian framework, evaluating the data based on the rule of stratigraphic superposition and the theoretical age-depth relationship for post-rift thermally subsiding basins (McKenzie, 1978). Results from sensitivity analyses using a synthetic dataset demonstrate that our program can successfully restore the stretching factor (β), the timing for the active rift to thermal subsidence transition (t_0), and age predictions for undated horizons.

As a case study, this model was implemented on the Tonian sedimentary succession in northeastern Svalbard, Norway, which is one of the best preserved and most complete successions of this time interval. We first present two new geochronological constraints for this succession: 1) a Re-Os age of 791.1 ± 4.9 Ma from the Svanbergfjellet Formation of the Akademikerbreen Group, and 2) a detrital zircon U-Pb CA-TIMS maximum deposition age of 879.91 ± 0.63 / 0.67 / 1.11 Ma for the Bogen Member of the Kingbreen Formation, Veteranen Group. By only using age constraints from the Svalbard succession itself, our model returns posterior distributions of $\beta = 1.29^{+0.08}_{-0.06}$ and $t_0 = 840.40^{+18.64}_{-23.61}$ Ma for the base of the Akademikerbreen Group. The results from this case study are broadly in agreement with the results from Halverson et al. (2022), albeit with larger uncertainties. We contribute this to the smaller number of assumptions that our model makes in both the model design and the selection of non-correlated age constraints. The rifting conditions (β and t_0) and subsidence history predicted by our model provide support for renewed extension in the Eastern basement province of Svalbard, likely within the latest Ediacaran–early Cambrian.

CRediT authorship contribution statement

Tianran Zhang: Conceptualization, Formal analysis, Methodology, Software, Validation, Visualization, Writing – original draft, Writing – review & editing. **C. Brenhin Keller:** Methodology, Software, Validation, Writing – review & editing. **Mark J. Hoggard:** Methodology, Writing – review & editing. **Alan D. Rooney:** Investigation, Resources, Writing – review & editing. **Galen P. Halverson:** Resources, Writing – review & editing. **Kristin D. Bergmann:** Investigation, Resources. **James L. Crowley:** Investigation, Writing – review & editing. **Justin V. Strauss:** Conceptualization, Investigation, Methodology, Resources, Supervision, Visualization, Writing – original draft, Writing – review & editing.

Declaration of competing interest

The authors declare that they have no known competing financial interests or personal relationships that could have appeared to influence the work reported in this paper.

Data availability

The raw data have been uploaded at the Attach File step as “Supplementary data”.

Acknowledgements

We thank the donors of the American Chemical Society Petroleum Research Fund for support of this research (58780-DNI8 awarded to JVS). This research was also supported by: National Geographic grant CP-129R-17 awarded to JVS; National Science Foundation (NSF) grants EAR-1929593 and EAR-1929597 awarded to JVS and ADR, respectively; and Australian Research Council Discovery Early Career Research Award (DE220101519) awarded to MH. We thank the Sysslemannen of Svalbard for sampling permits (RIS-ID 6867 and RIS-ID 11035), as well as T. Mackey, N. Tosca, A. Millikin, T. Gibson, and R. Anderson for help in the field. The thoughtful reviews by Matt Malkowski and an anonymous reviewer, as well as the editorial handling by Alex Webb, are much appreciated.

Appendix A. Supplementary material

Supplementary material related to this article can be found online at https://doi.org/10.1016/j.epsl.2023.118317.

References

Allaby, M. (Ed.), 2008. A Dictionary of Earth Sciences, A Dictionary of Earth Sciences. Oxford University Press. https://doi.org/10.1093/acref/9780199211944.001.0001.

Allen, P.A., Allen, J.R., 2013. Basin Analysis: Principles and Application to Petroleum Play Assessment. John Wiley & Sons.

Beaumont, C., Keen, C.E., Boutilier, R., 1982. On the evolution of rifted continental margins: comparison of models and observations for the Nova Scotian margin. Geophys. J. Int. 70, 667–715. https://doi.org/10.1111/j.1365-246X.1982.tb05979.x.

Blaauw, M., Christen, J.A., 2011. Flexible paleoclimate age-depth models using an autoregressive gamma process. Bayesian Anal. 6, 457–474. https://doi.org/10.1214/11-BA618.

Bond, G.C., Kominz, M.A., 1984. Construction of tectonic subsidence curves for the early Paleozoic miogeocline, southern Canadian Rocky Mountains: implications for subsidence mechanisms, age of breakup, and crustal thinning. Geol. Soc. Am. Bull. 95, 155–173. https://doi.org/10.1130/0016-7606(1984)95<155:COTSCF>2.0.CO;2.

Bond, G.C., Kominz, M.A., Devlin, W.J., 1983. Thermal subsidence and eustasy in the Lower Palaeozoic miogeocline of western North America. Nature 306, 775–779. https://doi.org/10.1038/306775a0.

Cawood, P.A., McCausland, P.J.A., Dunning, G.R., 2001. Opening Iapetus: constraints from the Laurentian margin in Newfoundland. Geol. Soc. Am. Bull. 113, 443–453. https://doi.org/10.1130/0016-7606(2001)113<0443:OICFTL>2.0.CO;2.

Cawood, P.A., Nemchin, A.A., Strachan, R., Prave, T., Krabbendam, M., 2007. Sedimentary basin and detrital zircon record along East Laurentia and Baltica during assembly and breakup of Rodinia. J. Geol. Soc. 164, 257–275. https://doi.org/10.1144/0016-76492006-115.

Cochran, J.R., 1983. Effects of finite rifting times on the development of sedimentary basins. Earth Planet. Sci. Lett. 66, 289–302. https://doi.org/10.1016/0012-821X(83)90142-5.

Cohen, P.A., Strauss, J.V., Rooney, A.D., Sharma, M., Tosca, N., 2017. Controlled hydroxyapatite biomineralization in an ∼810 million-year-old unicellular eukaryote. Sci. Adv. 3, e1700095. https://doi.org/10.1126/sciadv.1700095.

Coward, M.P., 1986. Heterogeneous stretching, simple shear and basin development. Earth Planet. Sci. Lett. 80, 325–336. https://doi.org/10.1016/0012-821X(86)90114-7.

Davis, M., Kusznir, N., 2004. 4. Depth-Dependent Lithospheric Stretching at Rifted Continental Margins. In: Karner, G., Taylor, B., Driscoll, N., Kohlstedt, D. (Eds.), Rheology and Deformation of the Lithosphere at Continental Margins. Columbia University Press, New York Chichester, West Sussex, pp. 92–137. https://doi.org/10.7312/karn12738-005.

Faehnrich, K., McClelland, W.C., Webb, L., Hadlari, T., Kośmińska, K., Strauss, J.V., in press. Late Ediacaran–early Cambrian rifting along the northern margin of Laurentia: constraints from the Yelverton Formation of Ellesmere Island, Canada. Can. J. Earth Sci.

Flood, B., Gee, D., Hjelle, A., Siggerud, T., Winsnes, T., 1969. The Geology of Nordaustlandet, northern and central parts.

Fortey, R.A., Bruton, D.L., 1973. Cambrian-Ordovician Rocks Adjacent to Hinlopenstretet, North Ny Friesland, Spitsbergen. Geol. Soc. Am. Bull. 84, 2227–2242. https://doi.org/10.1130/0016-7606(1973)84<2227:CRATHN>2.0.CO;2.

Gee, D.G., Johansson, Å., Ohta, Y., Tebenkov, A.M., Krasil'şçhikov, A.A., Balashov, Y.A., Larionov, A.N., Gannibal, L.F., Ryungenen, G.I., 1995. Grenvillian basement and a major unconformity within the Caledonides of Nordaustlandet, Svalbard. Precambrian Res. 70, 215–234. https://doi.org/10.1016/0301-9268(94)00041-O.

Gee, D.G., Teben'kov, A.M., 2004. Svalbard: a fragment of the Laurentian margin. In: Geological Society, London, Memoirs, vol. 30, pp. 191–206. https://doi.org/10.1144/GSL.MEM.2004.030.01.16.

Gibson, T.M., Millikin, A.E.G., Anderson, R.P., Myrow, P.M., Rooney, A.D., Strauss, J.V., 2021. Tonian deltaic and storm-influenced marine sedimentation on the edge of Laurentia: the Veteranen Group of northeastern Spitsbergen, Svalbard. Sediment. Geol. 426, 106011. https://doi.org/10.1016/j.sedgeo.2021.106011.

Giles, M.R., Indrelid, S.L., James, D.M.D., 1998. Compaction — the great unknown in basin modelling. In: Geological Society, London, Special Publications, vol. 141, pp. 15–43. https://doi.org/10.1144/GSL.SP.1998.141.01.02.

Gobbett, D.J., Wilson, C.B., 1960. The Oslobreen Series, Upper Hecla Hoek of Ny Friesland, Spitsbergen. Geol. Mag. 97, 441–457. https://doi.org/10.1017/S0016756800061835.

Halverson, G.P., Hoffman, P.F., Schrag, D.P., Maloof, A.C., Rice, A.H.N., 2005. Toward a Neoproterozoic composite carbon-isotope record. Geol. Soc. Am. Bull. 117, 1181–1207. https://doi.org/10.1130/B25630.1.

Halverson, G.P., Kunzmann, M., Strauss, J.V., Maloof, A.C., 2018a. The Tonian-Cryogenian transition in Northeastern Svalbard. In: Descent into the Cryogenian. Precambrian Res. 319, 79–95. https://doi.org/10.1016/j.precamres.2017.12.010.

Halverson, G.P., Maloof, A.C., Schrag, D.P., Dudás, F.Ö., Hurtgen, M., 2007. Stratigraphy and geochemistry of a ca 800 Ma negative carbon isotope interval in northeastern Svalbard. In: Precambrian Chemostratigraphy. Chem. Geol. 237, 5–27. https://doi.org/10.1016/j.chemgeo.2006.06.013.

Halverson, G.P., Porter, S.M., Gibson, T.M., 2018b. Dating the late Proterozoic stratigraphic record. Emerg. Top. Life Sci. 2, 137–147. https://doi.org/10.1042/ETLS20170167.

Halverson, G.P., Shen, C., Davies, J.H.F.L., Wu, L., 2022. A Bayesian approach to inferring depositional ages applied to a late Tonian reference section in Svalbard. Front. Earth Sci. 10. https://doi.org/10.3389/feart.2022.798739.

Harland, W.B., 1997. Proto-basement in Svalbard. Polar Res. 16, 123–147. https://doi.org/10.3402/polar.v16i2.6631.

Harland, W.B., Wilson, C.B., 1956. The Hecla Hoek Succession in Ny Friesland, Spitsbergen. Geol. Mag. 93, 265–286. https://doi.org/10.1017/S0016756800066693.

Haslett, J., Parnell, A., 2008. A simple monotone process with application to radiocarbon-dated depth chronologies. J. R. Stat. Soc., Ser. C, Appl. Stat. 57, 399–418. https://doi.org/10.1111/j.1467-9876.2008.00623.x.

Herrington, P.M., Fairchild, I.J., 1989. Carbonate shelf and slope facies evolution prior to Vendian galciation, central East Greenland. In: The Caledonides geology of Scandinavia, pp. 263–273. https://doi.org/10.1007/978-94-009-2549-6_22. Conference dedicated to the Memory of Dr Sven Foyn.

Hoffman, P.F., Halverson, G.P., Domack, E.W., Maloof, A.C., Swanson-Hysell, N.L., Cox, G.M., 2012. Cryogenian glaciations on the southern tropical paleomargin of Laurentia (NE Svalbard and East Greenland), and a primary origin for the upper Russøya (Islay) carbon isotope excursion. Precambrian Res. 206–207, 137–158. https://doi.org/10.1016/j.precamres.2012.02.018.

Hölzel, M., Faber, R., Wagreich, M., 2008. DeCompactionTool: software for subsidence analysis including statistical error quantification. Comput. Geosci. 34, 1454–1460. https://doi.org/10.1016/j.cageo.2008.01.002.

Huismans, R.S., Beaumont, C., 2014. Rifted continental margins: the case for depth-dependent extension. Earth Planet. Sci. Lett. 407, 148–162. https://doi.org/10.1016/j.epsl.2014.09.032.

Japsen, P., Green, P.F., Nielsen, L.H., Rasmussen, E.S., Bidstrup, T., 2007. Mesozoic–Cenozoic exhumation events in the eastern North Sea Basin: a multi-disciplinary study based on palaeothermal, palaeoburial, stratigraphic and seismic data. Basin Res. 19, 451–490. https://doi.org/10.1111/j.1365-2117.2007.00329.x.

Jarvis, G.T., McKenzie, D.P., 1980. Sedimentary basin formation with finite extension rates. Earth Planet. Sci. Lett. 48, 42–52. https://doi.org/10.1016/0012-821X(80)90168-5.

Johansson, Å., Gee, D.G., Larionov, A.N., Ohta, Y., Tebenkov, A.M., 2005. Grenvillian and Caledonian evolution of eastern Svalbard – a tale of two orogenies. Terra Nova 17, 317–325. https://doi.org/10.1111/j.1365-3121.2005.00616.x.

Johnstone, S.A., Schwartz, T.M., Holm-Denoma, C.S., 2019. A stratigraphic approach to inferring depositional ages from detrital geochronology data. Front. Earth Sci. 7, 57. https://doi.org/10.3389/feart.2019.00057.

Keller, C.B., 2018. Chron.jl: A Bayesian framework for integrated eruption age and age-depth modelling. https://doi.org/10.17605/osf.io/TQX3F.

Knoll, A.H., Hayes, J.M., Kaufman, A.J., Swett, K., Lambert, I.B., 1986. Secular variation in carbon isotope ratios from Upper Proterozoic successions of Svalbard and East Greenland. Nature 321, 832–838. https://doi.org/10.1038/321832a0.

Knoll, A.H., Swett, K., 1987. Micropaleontology across the Precambrian—Cambrian boundary in Spitsbergen. J. Paleontol. 61, 898–926. https://doi.org/10.1017/S0022336000029292.

Kooi, H., Hettema, M., Cloetingh, S., 1991. Lithospheric dynamics and the rapid Pliocene-quaternary subsidence phase in the southern North Sea basin. Tectonophysics 192, 245–259. https://doi.org/10.1016/0040-1951(91)90102-X.

Kulling, O., 1934. Part XI. The »Hecla Hoek Formation» round Hinlopenstredet: NW North-East Land and NE West Spitsbergen. Geogr. Ann. 16, 161–254. https://doi.org/10.1080/20014422.1934.11880584.

Kusznir, N.J., Marsden, G., Egan, S.S., 1991. A flexural-cantilever simple-shear/pure-shear model of continental lithosphere extension: applications to the Jeanne d'Arc Basin, Grand Banks and Viking Graben, North Sea. In: Geological Society, London, Special Publications, vol. 56, pp. 41–60. https://doi.org/10.1144/GSL.SP.1991.056.01.04.

Levy, M., Christie-Blick, N., 1991. Tectonic subsidence of the early Paleozoic passive continental margin in eastern California and southern Nevada. Geol. Soc. Am. Bull. 103, 1590–1606. https://doi.org/10.1130/0016-7606(1991)103<1590:TSOTEP>2.3.CO;2.

Macdonald, F.A., Schmitz, M.D., Crowley, J.L., Roots, C.F., Jones, D.S., Maloof, A.C., Strauss, J.V., Cohen, P.A., Johnston, D.T., Schrag, D.P., 2010. Calibrating the Cryogenian. Science 327, 1241–1243. https://doi.org/10.1126/science.1183325.

MacLennan, S., Park, Y., Swanson-Hysell, N., Maloof, A., Schoene, B., Gebreslassie, M., Antilla, E., Tesema, T., Alene, M., Haileab, B., 2018. The arc of the Snowball: U-Pb dates constrain the Islay anomaly and the initiation of the Sturtian glaciation. Geology 46, 539–542. https://doi.org/10.1130/G40171.1.

Maloof, A.C., Halverson, G.P., Kirschvink, J.L., Schrag, D.P., Weiss, B.P., Hoffman, P.F., 2006. Combined paleomagnetic, isotopic, and stratigraphic evidence for true polar wander from the Neoproterozoic Akademikerbreen Group, Svalbard, Norway. Geol. Soc. Am. Bull. 118, 1099–1124. https://doi.org/10.1130/B25892.1.

McKenzie, D., 1978. Some remarks on the development of sedimentary basins. Earth Planet. Sci. Lett. 40, 25–32. https://doi.org/10.1016/0012-821X(78)90071-7.

Meng, Q.-R., Wei, H.-H., Qu, Y.-Q., Ma, S.-X., 2011. Stratigraphic and sedimentary records of the rift to drift evolution of the northern North China craton at the Paleo- to Mesoproterozoic transition. In: Precambrian Geology and Tectonic Evolution of the North China Craton. Gondwana Res. 20, 205–218. https://doi.org/10.1016/j.gr.2010.12.010.

Millikin, A.E.G., Strauss, J.V., Halverson, G.P., Bergmann, K.D., Tosca, N.J., Rooney, A.D., 2022. Calibrating the Russøya excursion in Svalbard, Norway, and implications for Neoproterozoic chronology. Geology 50, 506–510. https://doi.org/10.1130/G49593.1.

Pedersen, T., Ro, H.E., 1992. Finite duration extension and decompression melting. Earth Planet. Sci. Lett. 113, 15–22. https://doi.org/10.1016/0012-821X(92)90208-D.

Pu, J.P., Macdonald, F.A., Schmitz, M.D., Rainbird, R.H., Bleeker, W., Peak, B.A., Flowers, R.M., Hoffman, P.F., Rioux, M., Hamilton, M.A., 2022. Emplacement of the Franklin large igneous province and initiation of the Sturtian Snowball Earth. Sci. Adv. 8, eadc9430. https://doi.org/10.1126/sciadv.adc9430.

Ramsey, C.B., 2008. Deposition models for chronological records. In: INTegration of Ice-Core, Marine and Terrestrial Records (INTIMATE): Refining the Record of the Last Glacial-Interglacial Transition. Quat. Sci. Rev. 27, 42–60. https://doi.org/10.1016/j.quascirev.2007.01.019.

Rooney, A.D., Macdonald, F.A., Strauss, J.V., Dudás, F.Ö., Hallmann, C., Selby, D., 2014. Re-Os geochronology and coupled Os-Sr isotope constraints on the Sturtian snowball Earth. Proc. Natl. Acad. Sci. 111, 51–56. https://doi.org/10.1073/pnas.1317266110.

Sandelin, S., Tebenkov, A.M., Gee, D.G., 2001. The stratigraphy of the lower part of the Neoproterozoic Murchisonfjorden Supergroup in Nordaustlandet, Svalbard. Gff 123, 113–127. https://doi.org/10.1080/11035890101232113.

Sandford, K.S., 1926. The Geology of North-East Land (Spitsbergen). Q. J. Geol. Soc. 82, 615–665. https://doi.org/10.1144/GSL.JGS.1926.082.01-04.33.

Sclater, J.G., Christie, P.a.F., 1980. Continental stretching: an explanation of the Post-Mid-Cretaceous subsidence of the central North Sea Basin. J. Geophys. Res., Solid Earth 85, 3711–3739. https://doi.org/10.1029/JB085iB07p03711.

Shields, G.A., Strachan, R.A., Porter, S.M., Halverson, G.P., Macdonald, F.A., Plumb, K.A., de Alvarenga, C.J., Banerjee, D.M., Bekker, A., Bleeker, W., Brasier, A., Chakraborty, P.P., Collins, A.S., Condie, K., Das, K., Evans, D.A.D., Ernst, R., Fallick, A.E., Frimmel, H., Fuck, R., Hoffman, P.F., Kamber, B.S., Kuznetsov, A.B., Mitchell, R.N., Poiré, D.G., Poulton, S.W., Riding, R., Sharma, M., Storey, C., Stueeken, E., Tostevin, R., Turner, E., Xiao, S., Zhang, S., Zhou, Y., Zhu, M., 2021. A template for an improved rock-based subdivision of the pre-Cryogenian timescale. J. Geol. Soc. 179, jgs2020-222. https://doi.org/10.1144/jgs2020-222.

Skogseid, J., Planke, S., Faleide, J.I., Pedersen, T., Eldholm, O., Neverdal, F., 2000. NE Atlantic continental rifting and volcanic margin formation. In: Geological Society, London, Special Publications, vol. 167, pp. 295–326. https://doi.org/10.1144/GSL.SP.2000.167.01.12.

Smith, M.P., Rasmussen, J.A., 2008. Cambrian–Silurian development of the Laurentian margin of the Iapetus Ocean in Greenland and related areas. In: Higgins, A.K., Gilotti, J.A., Smith, M.P. (Eds.), The Greenland Caledonides: Evolution of the Northeast Margin of Laurentia. Geological Society of America. https://doi.org/10.1130/2008.1202(06).

Smoliar, M.I., Walker, R.J., Morgan, J.W., 1996. Re-Os Ages of Group IIA, IIIA, IVA, and IVB Iron Meteorites. Science 271, 1099–1102. https://doi.org/10.1126/science.271.5252.1099.

Strauss, J.V., Rooney, A.D., Macdonald, F.A., Brandon, A.D., Knoll, A.H., 2014. 740 Ma vase-shaped microfossils from Yukon, Canada: implications for Neoproterozoic chronology and biostratigraphy. Geology 42, 659–662. https://doi.org/10.1130/G35736.1.

Surlyk, F., 1991. Tectonostratigraphy of North Greenland. Bull. Grønl. Geol. Unders. 160, 25–47. https://doi.org/10.34194/bullggu.v160.6712.

Swanson-Hysell, N.L., Maloof, A.C., Condon, D.J., Jenkin, G.R.T., Alene, M., Tremblay, M.M., Tesema, T., Rooney, A.D., Haileab, B., 2015. Stratigraphy and geochronology of the Tambien Group, Ethiopia: evidence for globally synchronous carbon isotope change in the Neoproterozoic. Geology 43, 323–326. https://doi.org/10.1130/G36347.1.

Swanson-Hysell, N.L., Maloof, A.C., Kirschvink, J.L., Evans, D.A.D., Halverson, G.P., Hurtgen, M.T., 2012. Constraints on Neoproterozoic paleogeography and Paleozoic orogenesis from paleomagnetic records of the Bitter Springs Formation, Amadeus Basin, central Australia. Am. J. Sci. 312, 817–884. https://doi.org/10.2475/08.2012.01.

Swett, K., 1981. Cambro-Ordovician strata in Ny Friesland, Spitsbergen and their palaeotectonic significance. Geol. Mag. 118, 225–250. https://doi.org/10.1017/S001675680003572X.

VanderLeest, R.A., Fosdick, J.C., Malkowski, M.A., Romans, B.W., Ghiglione, M.C., Schwartz, T.M., Sickmann, Z.T., 2022. Tectonic subsidence modeling of diachronous transition from backarc to retroarc basin development and uplift during Cordilleran orogenesis, Patagonian-Fuegian Andes. Tectonics 41, e2021TC006891. https://doi.org/10.1029/2021TC006891.

Wala, V.T., Ziemniak, G., Majka, J., Faehnrich, K., McClelland, W.C., Meyer, E.E., Manecki, M., Bazarnik, J., Strauss, J.V., 2021. Neoproterozoic stratigraphy of the Southwestern Basement Province, Svalbard (Norway): Constraints on the Proterozoic-Paleozoic evolution of the North Atlantic-Arctic Caledonides. Precambrian Res. 358, 106138. https://doi.org/10.1016/j.precamres.2021.106138.

Wernicke, B., 1981. Low-angle normal faults in the Basin and Range Province: nappe tectonics in an extending orogen. Nature 291, 645–648. https://doi.org/10.1038/291645a0.

Williams, H., Hiscott, R.N., 1987. Definition of the lapetus rift-drift transition in western Newfoundland. Geology 15, 1044–1047. https://doi.org/10.1130/0091-7613(1987)15<1044:DOTLRT>2.0.CO;2.

Yonkee, W.A., Dehler, C.D., Link, P.K., Balgord, E.A., Keeley, J.A., Hayes, D.S., Wells, M.L., Fanning, C.M., Johnston, S.M., 2014. Tectono-stratigraphic framework of Neoproterozoic to Cambrian strata, west-central U.S.: Protracted rifting, glaciation, and evolution of the North American Cordilleran margin. Earth-Sci. Rev. 136, 59–95. https://doi.org/10.1016/j.earscirev.2014.05.004.

Zhang, T., Keller, C.B., Strauss, J.V., 2023. SubsidenceChron.jl. https://doi.org/10.17605/OSF.IO/ZW5GA.